JACS
JOURNAL OF THE AMERICAN CHEMICAL SOCIETY
Article
pubs.acs.org/JACS

Synthesis and Biological Evaluation of Dimeric Furanoid Macroheterocycles: Discovery of New Anticancer Agents

K. C. Nicolaou,*[,†] Christian Nilewski,[†] Christopher R. H. Hale,[†] Christopher F. Ahles,[‡] Chiao An Chiu,[‡] Christian Ebner,[‡] Abdelatif ElMarrouni,[†] Lifeng Yang,[§] Katherine Stiles,[§] and Deepak Nagrath[§]

[†]Department of Chemistry, BioScience Research Collaborative and [§]Department of Chemical and Biomolecular Engineering, Rice University, 6100 Main Street, Houston, Texas 77005, United States

[‡]Department of Chemistry, The Scripps Research Institute, 10550 North Torrey Pines Road, La Jolla, California 92037, United States

Supporting Information

ABSTRACT: A recently developed dimerization/macrocyclization was employed to synthesize a series of macroheterocycles which were biologically evaluated, leading to the discovery of a number of potent cytotoxic agents (e.g., **27**: GI_{50} = 51 nM against leukemia CCRF-CEM cell line; **29**: GI_{50} = 99 nM against melanoma MDA-MB-435 cell line). Further biological studies support an apoptosis mechanism of action for these compounds involving deregulation of the tricarboxylic acid cycle activity and suppression of mitochondrial function in cancer cells.

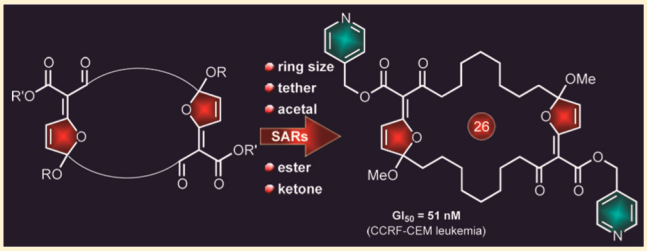

1. INTRODUCTION

Historically, naturally occurring macrocyclic compounds feature prominently in the repertoire of biologically and medically important molecules.[1] More recently, synthetic macrocycles have also been recognized as useful lead compounds, drug candidates, and approved drugs.[2] As part of a program directed toward synthetic technologies to construct such macrocycles,[3] we recently developed a cerium(IV)-mediated oxidative macrocyclization of furanoid β-ketoesters (**A**) to yield, depending on the conditions, either monomeric (**B**) or dimeric (**C**) macroheterocycles (see Scheme 1).[4] In this article we report the discovery of potent antitumor agents through studies made possible by application of this process. Specifically, we describe the synthesis of a series of macroheterocycles from which we identified a lead compound whose optimization led to the discovery of several potent cytotoxic compounds active against a number of cancer cell lines at nanomolar concentrations.

Scheme 1. Synthesis of Monomeric and Dimeric Macroheterocycles[4,a]

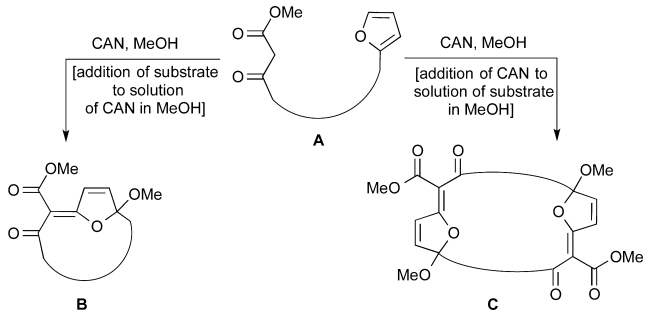

[a]CAN = cerium(IV) ammonium nitrate.

2. RESULTS AND DISCUSSION

2.1. Initial Lead Compounds and Synthesis of Second-Generation Dimeric Macroheterocycles. Our initial investigations began with submission of the originally synthesized compounds **1**–**12**[4] (Table 1) to the NCI 60 cell line panel for in vitro cytotoxicity screening.[5] As seen in Table 3, neither the uncyclized furanoid β-ketoester **1** nor the monomeric macroheterocycles **2**–**4** displayed significant cytotoxicity against a variety of cell lines (see Table 3 for NCI 1-dose mean growth values).

In contrast, dimeric macroheterocycles **5**–**12** exhibited interesting cytotoxic profiles and a revealing ring size effect on potency. Thus, depending on their ring size, these compounds showed potencies down to submicromolar ranges, with **9** [n = 4, 26-membered ring; GI_{50} = 0.336 μM against HCT-116 (colon cancer)] and **10** [n = 5, 28-membered ring; GI_{50} = 0.676 μM against HCT-116 (colon cancer)] being the most potent (see Table 3). Notably, the smallest (**5**, 18-membered) and the largest (**12**, 40-membered) ring dimers were found to be the least active (see Table 3).

In light of these results, we set dimeric macrocycle **9** (26-membered) as a lead compound and proceeded to modify its structural motifs [i.e., (i) acetal side-chain; (ii) tether linker; (iii) ketone moiety; and (iv) ester side-chain] in order to gather structure–activity relationships (SARs) and optimize its

Received: January 9, 2015
Published: April 1, 2015

DOI: 10.1021/jacs.5b00141
J. Am. Chem. Soc. 2015, 137, 4766–4770

Table 1. Previously Synthesized β-Ketoester Precursor 1 (a), Monomeric Macroheterocycles 2–4 (b), and Dimeric Macroheterocycles 5–12 (c) Selected for Initial Biological Evaluation

a) furanoid β-ketoesters

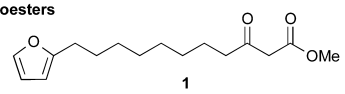

1

b) monomeric macroheterocycles

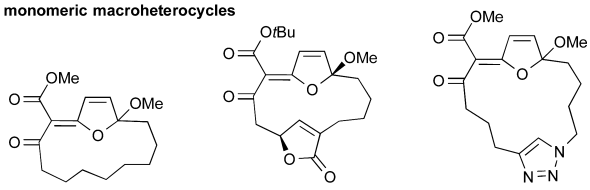

2 3 4

c) dimeric macroheterocycles

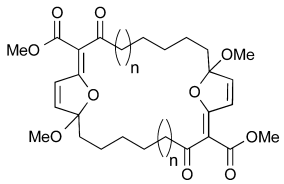

Compound	n	Ring size
5	0	[18]
6	1	[20]
7	2	[22]
8	3	[24]
9	4	[26]
10	5	[28]
11	6	[30]
12	11	[40]

potency. Table 2 shows the preparation of a number of dimeric macrocycles with varying tether linkers, ring sizes, and acetal side-chains (**13**–**18**, X, Y = CH_2, O, or SO_2; R = Me or Et, 10–38% yield, unoptimized; see Supporting Information for details).

Table 2. Synthesis of Dimeric Macroheterocycles with Varying Ring Sizes, Tethers, and Acetal Side-Chains (13–18)

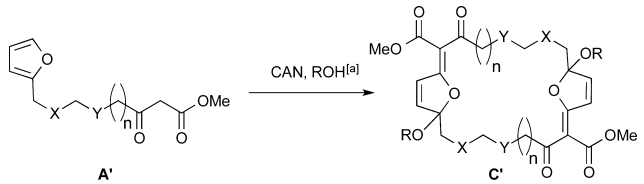

A' C'

compound	*n*	ring size	X	Y	R	yield (%)
13	3	[24]	CH_2	CH_2	Et	38
14	4	[26]	CH_2	CH_2	Et	11
15	4	[26]	CH_2	O	Me	10
16	4	[26]	CH_2	SO_2	Me	13
17	4	[26]	O	CH_2	Me	11
18	4	[26]	SO_2	CH_2	Me	12

[a]Addition of CAN to solution of substrate in MeOH or EtOH (see Supporting Information for details).

In addition to these compounds, the 26-membered macrocycles **19** (diol, mixture of diastereoisomers, prepared from **9** by reduction), **21** (bis-carboxylic acid, prepared from **9** by LiOH/H_2O hydrolysis), and **24**–**32** (bis-esters, prepared from **21**, by reaction with K_2CO_3 and the corresponding bromide or mesylate) were added to the collection of macroheterocycles (see Scheme 2).

The 24-membered macrocycles **20** and **20a** (bis-carboxylic acids, prepared from **8** and **13**, respectively) and **22** and **23** (bis-benzyl ethers with methyl and ethyl acetal side-chains, respectively) were also synthesized (see Scheme 2) for biological screening comparison purposes. All macrocycles

Scheme 2. Synthesis of Dimeric Macroheterocycles with Varying Substituents on the Macrocycle and Ester Side-Chains[a]

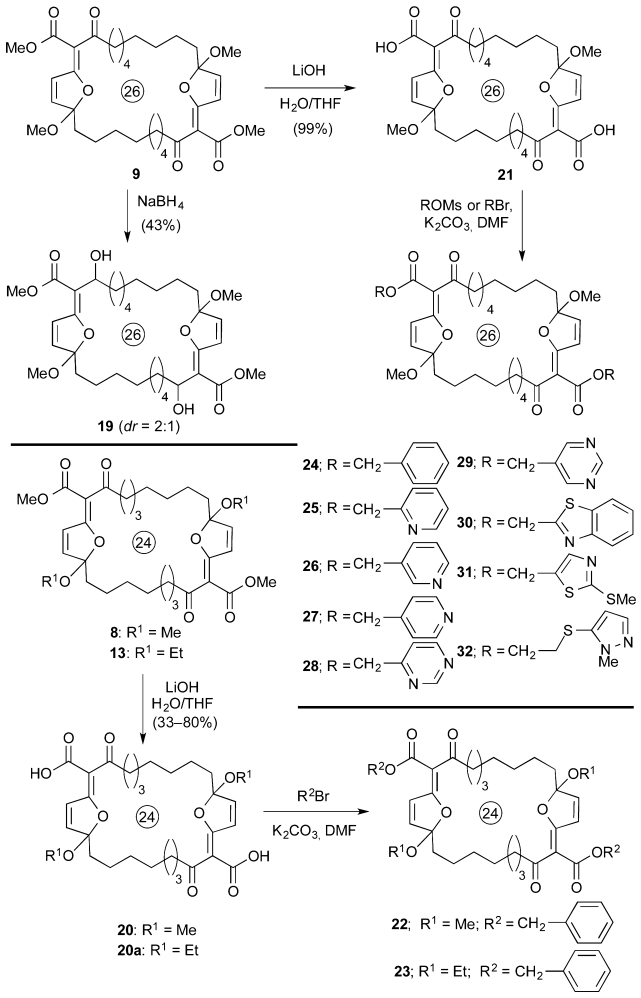

[a]See Supporting Information for details.

were obtained as diastereoisomeric mixtures (*syn*- and *anti*-acetal side-chains, ca. 1:1 d.r.) and tested as such, except for bis-pyridine **26** which was not only tested as a diastereomeric mixture, but also yielded to chromatographic separation of its two isomeric forms (i.e., *syn*-**26** and *anti*-**26**, Figure 1). Pleasantly, the less polar isomer (silica gel, CH_2Cl_2:acetone 3:2) crystallized in suitable form (mp 139–140 °C, MeOH/CH_2Cl_2) for X-ray crystallographic analysis, revealing its *anti*-configuration (*anti*-**26**) and leading, by deduction, to the assignment of the *syn*-configuration for the other isomer (*syn*-**26**) (see ORTEP representation, Figure 1).[6]

2.2. Biological Evaluation of Synthesized Dimeric Macroheterocycles. Synthesized compounds were submitted to the NCI 60 cell line panel for in vitro cytotoxicity evaluation, and the data obtained from these studies are shown in Tables 3 and 4. Table 3 shows an overview of the one-dose mean growth inhibition (%) for all synthesized compounds and, for those that passed the initial one-dose screening test, the growth inhibition range (GI_{50}, μM) and the most sensitive cell line. As mentioned above, neither the precursor furanoid ketoester **1** nor any of the tested monomeric macroheterocycles (**2**–**4**) exhibited significant cytotoxicity in the one-dose mean growth assay (see Scheme 1 and Table 3). However, and with only few

DOI: 10.1021/jacs.5b00141
J. Am. Chem. Soc. 2015, 137, 4766–4770

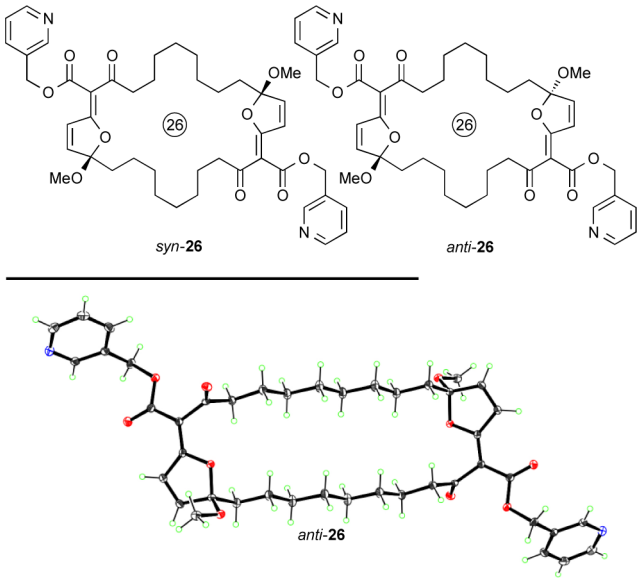

Figure 1. Molecular structures of diastereomerically pure pyridine analogues *syn*-**26** and *anti*-**26** (top) and ORTEP representation of *anti*-**26** (bottom). Thermal ellipsoids at 30% probability; gray = carbon, red = oxygen, blue = nitrogen, green = hydrogen.

exceptions, most of the 24- and 26-membered dimeric macrocycles exhibited moderate to strong cytotoxicities against a range of cell lines as summarized in Table 3.

With regard to the acetal side-chain, the methyl and ethyl groups led to comparable potencies (compare **8** with **13**, and **9** with **14**, Table 3). Interestingly, in most cases heteroatoms or heteroatom groups in the tethers (compare **15**, **16**, **17**, and **18** with **9**, Table 3) decreased the potencies of the macrocycles as did reduction of the two keto groups within the macrocyclic ring (compare **19** with **9**, Table 3). Modifications of the carboxylate side-chain also proved revealing. Thus, the 24- and 26-membered ring bis-carboxylic acids **20** and **21** exhibited only weak, if any, cytotoxicities (compare compounds **20** and **21** with **8** and **9**, respectively, Table 3) and so did the benzyl esters (**22**−**24**, see Table 3). In contrast, incorporation of heteroaromatic rings in the ester moieties resulted in the discovery of analogues with enhanced potencies compared to **9** as highlighted in Table 3 (compounds **25**, **26**, *syn*-**26**, and **27**−**29**). Interestingly, compounds **30** and **31** were found to be less active than the other heterocycle-containing esters. The most potent compounds were the pyridine- (**27**: GI_{50} = 51 nM against leukemia CCRF-CEM line) and pyrimidine- (**29**: GI_{50} = 99 nM against melanoma MDA-MB-435 line) containing compounds (see Table 3). It is also interesting to note that the syn-diastereoisomer of **26** (*syn*-**26**) proved more potent than its *anti*-counterpart (*anti*-**26**, see Table 3).

Table 4 displays the potencies of selected compounds against six cancer cell lines (BT-549 breast cancer, CCRF-CEM leukemia, MDA-MB-435 melanoma, SK-MEL-5 melanoma, LOX-IMVI melanoma, and RXF-393 renal cancer) of the NCI panel for comparison. As seen, several compounds featuring heterocycle-containing esters exhibited sub-200 nM potencies against these cell lines as highlighted in boxes in Table 4 (e.g., **25**: GI_{50} = 188 nM against melanoma LOX-IMVI; **26**: GI_{50} = 171 nM against breast cancer BT-549; *syn*-**26**: GI_{50} = 179 nM against melanoma SK-MEL-5; **27**: GI_{50} = 51.4 nM against leukemia CCRF-CEM, 121 nM against melanoma MDA-MB-435, and 107 nM against melanoma LOX-IMVI; and **29**: GI_{50} = 155 nM against melanoma LOX-IMVI and 99.0 nM against melanoma MDA-MB-435).

Table 3. Overview of Biological Evaluation of Select Monomeric and Dimeric Macroheterocycles

Compound	One dose (mean growth %)[a]	GI_{50} range (μM)[b]	Most sensitive cell line[c]
1	101.66	–	–
2	97.72	–	–
3	102.75	–	–
4	105.08	–	–
5	72.45	–	–
6	1.07	1.35–4.56	RXF-393, renal cancer
7	−20.32	1.10–3.77	HCT-116, colon cancer
8	−42.19	1.35–3.36	LOX IMVI, melanoma
9	−18.95	0.336–3.44	HCT-116, colon cancer
10	−13.92	0.676–4.93	HCT-116, colon cancer
11	53.70	1.82–>100	HCT-116, colon cancer
12	97.13	–	–
13	−38.07	0.270–2.93	HCT-116, colon cancer
14	−17.73	0.341–4.18	HCT-116, colon cancer
15	44.74	1.55–7.58	UO-31, renal cancer
16	85.74	–	–
17	−36.68	0.514–3.14	HCT-116, colon cancer
18	84.08	–	–
19	62.44	1.30–>100	PC-3, prostate cancer
20	98.94	–	–
21	100.39	–	–
22	54.71	0.701–>100	CCRF-CEM, leukemia
23	84.42	–	–
24	75.22	–	–
25	−20.40	0.188–1.69	LOX IMVI, melanoma
26	−51.65	0.171–0.501	BT-549, breast cancer
syn-**26**	−51.45	0.179–1.02	SK-MEL-5, melanoma
anti-**26**	−1.86	0.275–3.63	HCT-116, colon cancer
27	−33.49	0.051–2.03	CCRF-CEM, leukemia
28	−21.18	0.193–1.52	RXF-393, renal cancer
29	−32.03	0.099–1.30	MDA-MB-435, melanoma
30	64.15	–	–
31	29.79	0.439–70.0	HCT-116, colon cancer
32	−3.53	0.573–2.35	LOX IMVI, melanoma

[a]Growth percent at 10 μM vs negative control. [b]GI_{50}: Concentration required to inhibit growth by 50%. [c]See the Supporting Information for further details.

The lower potencies of the less lipophilic macrocycles **15**−**18** carrying heteroatoms in their tethers as well as diol **19** and bis-carboxylic acids **20** and **21** may be attributed to their diminished ability to penetrate the cell membrane. The higher potencies of the heteroaromatic-containing compounds **25**, **26**, *syn*-**26**, and **27**−**29** are presumably due to stronger binding to their receptor originating from their basic character, stacking, and ability to form H-bonds.

The ring size effect is intriguing and cannot be precisely rationalized without further experimentation. However, taken together with the fact that the monomeric macrocycles are devoid of activity, this effect may be pointing to two binding-sites within the biological target or interference with protein−protein interactions that require two pharmacophoric structural

DOI: 10.1021/jacs.5b00141
J. Am. Chem. Soc. 2015, 137, 4766−4770

Table 4. Comparison of GI_{50} Values of Compounds Against Selected Cancer Cell Lines (μM)[a]

Compound	BT-549 (breast)	CCRF-CEM (leukemia)	MDA-MB-435 (melanoma)	SK-MEL-5 (melanoma)	LOX-IMVI (melanoma)	RXF-393 (renal)
6	3.11	2.84	2.01	1.65	2.49	1.35
7	2.19	2.28	1.55	1.51	1.60	1.43
8	1.65	2.11	1.48	1.51	1.35	1.47
9	0.641	0.448	0.400	1.43	0.708	1.15
10	1.72	1.76	1.74	1.43	1.52	1.54
11	7.99	3.26	3.00	5.31	3.38	2.82
13	1.45	0.467	0.473	1.15	1.21	1.43
14	1.40	0.422	0.580	1.76	1.20	1.65
15	2.35	2.72	1.99	2.01	2.12	1.81
17	1.96	1.54	1.30	1.58	1.69	1.62
19	2.82	14.1	27.8	3.78	27.4	4.50
22	4.86	0.701	4.08	5.38	9.50	7.38
25	0.401	–	0.209	0.221	0.188	0.192
26	0.171	0.321	0.175	0.185	0.189	0.202
syn-**26**	0.278	–	0.199	0.179	0.205	0.188
anti-**26**	1.51	0.741	0.779	0.856	0.585	0.915
27	0.638	0.0514	0.121	0.247	0.107	0.277
28	0.225	0.251	0.194	–	0.211	0.193
29	0.188	0.196	0.0990	–	0.155	0.199
31	4.53	0.455	1.68	1.70	1.20	1.75
32	0.954	1.09	0.685	0.581	0.573	0.665

[a]See Supporting Information for further details.

motifs held apart at a certain distance. These structural motifs are almost certainly the furanoid dicarbonyl moieties as supported by the fact that reduction of the two endocyclic carbonyl groups leads to decreased activity (see **19**, Table 3).

2.3. Investigations Regarding the Mechanism of Action of Synthesized Dimeric Macroheterocycles. In order to ascertain whether these newly discovered antitumor agents act against drug-resistant cancer cells, we tested compounds **9** and **28** against ovarian cancer cells and cisplatin-resistant ovarian cancer cells and found them to be active at the GI_{50} range of 3.05−5.30 μM for **9** and 0.319−1.34 μM for **28**. Specifically, **9** and **28** exhibited activities against ovarian cancer line OVCAR3 (**9**: GI_{50} = 3.39 μM; **28**: 0.319 μM), SKOV3 (**9**: GI_{50} = 3.76 μM; **28**: 0.80 μM), OVCA420 (**9**: GI_{50} = 3.05 μM; **28**: 0.517 μM), OVCA429 (**9**: GI_{50} = 5.30 μM; **28**: 1.34 μM), IGROV1par (**9**: GI_{50} = 5.08 μM; **28**: 1.20 μM), and IGROV1 cP20 (**9**: GI_{50} = 4.48 μM; **28**: 0.783 μM) (see Supporting Information for further details). To probe the mechanism of action of these macroheterocycles, we investigated the effects of compound **28** on the energetics of cancer cells and glycolysis.[7] Thus, **28** was found to decrease basal oxygen consumption rate (OCR) for SKOV3 (control: 3.4 pmol/min/μg protein; **28**: 1.2 pmol/min/μg protein, see Figure 2a) and ATP-Linked OCR (control: 2.6 pmol/min/μg protein; **28**: 0.55 pmol/min/μg protein, see Figure 2b) as well

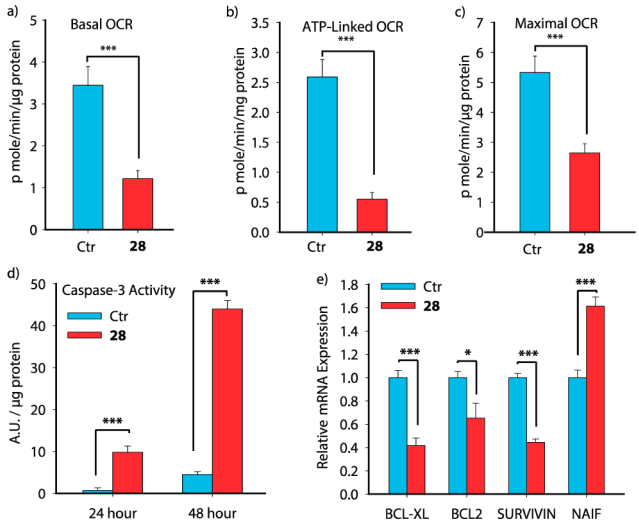

Figure 2. Effects of macroheterocycle **28** on the energetics and glycolysis in ovarian cancer cells. (a) Basal mitochondrial oxygen consumption rate (OCR). (b) ATP-linked OCR in the presence of oligomycin, an inhibitor of mitochondrial complex V. (c) Maximal OCR in the presence of carbonyl cyanide-4-(trifluoromethoxy)-phenylhydrazone, a mitochondrial uncoupler. Effects of macroheterocycle **28** on apoptosis. (d) Caspase-3 activity. (e) Expression of apoptosis related genes. Ctr = control, *: $p \leq 0.05$, **: $p \leq 0.01$, ***: $p \leq 0.001$ (see Supporting Information for further details).

as maximal OCR (control: 5.3 pmol/min/μg protein; **28**: 2.6 pmol/min/μg protein, see Figure 2c), suggesting that these agents induce modulation of mitochondrial dysfunction in cancer cells. Furthermore, macroheterocycle **28** reduced turnover of ATP and decreased its capacity to oxidize as measured by the calculated respiratory control ratio[8] (SKOV3 control: 6.0; **28**: 3.0, see Supporting Information). We also measured the extent of glycolysis in cancer cells in the presence of **28**, revealing an increase of the glucose uptake (**28** increased glucose uptake by 51% for SKOV3, 36% for OVCA429, 34% for IGROV1, and 43% for OVCAR3, see Supporting Information for further details) and lactate secretion (**28** increased lactate secretion by 26% for SKOV3, 34% for OVCA429, 14% for IGROV1, and 25% for OVCAR3, see Supporting Information for further details). The observed increase in glucose uptake and lactate secretion indicates hyperglycolysis.[9] These results support the hypothesis that these macroheterocycles exert their cancer cell cytotoxicity through deregulation of mitochondrial tricarboxylic acid cycle activity and suppression of mitochondrial function. In addition, the reduction of the expression level of mitochondrial complex II (SDHB), complex III (UQCRH and CYTB), and complex V (ATPsyn F1) genes in the presence of macroheterocycle **28** confirmed that these compounds induce mitochondrial dysfunction (see Supporting Information for further details).

Mitochondrial dysfunction may induce the release of cytochrome C, which eventually activates the apoptosis pathway.[10] Further studies proved that **28** dramatically increased caspase-3 activity indicating apoptosis (see Figure 2d). This hypothesis was validated by the observed decrease of expression of the apoptosis inhibitor proteins BCL-XL, BCL2, and survivin and increase of expression of the nuclear apoptosis induced factor (NAIF) (see Figure 2e).[11] These results strongly suggest that these macroheterocycles act by induction of

DOI: 10.1021/jacs.5b00141
J. Am. Chem. Soc. 2015, 137, 4766−4770

mitochondrial dysfunction activating a cascade of signaling events leading to cell death of cancer cells through apoptosis.

3. CONCLUSION

In conclusion, we employed a newly developed method for the synthesis of dimeric macroheterocycles to discover a series of potent antitumor agents. Further optimization of the discovered lead compounds may lead to drug candidates and payloads for antibody drug conjugates directed toward personalized and targeted cancer chemotherapy.

■ ASSOCIATED CONTENT

Supporting Information

Experimental procedures and characterization data for all compounds. This material is available free of charge via the Internet at http://pubs.acs.org.

■ AUTHOR INFORMATION

Corresponding Author

*kcn@rice.edu

Notes

The authors declare no competing financial interest.

■ ACKNOWLEDGMENTS

Dedicated to Professor H. M. R. Hoffmann on the occasion of his 80th birthday. Financial support for this work was provided by the National Institutes of Health, USA (grant AI055475), the Skaggs Institute for Research, the Cancer Prevention & Research Institute of Texas (CPRIT), and The Welch Foundation. Fellowships to C.N. (Feodor Lynen Research Fellowship, Alexander von Humboldt Foundation), C.R.H.H. (NSF Graduate Research Fellowship), C.E. (Otto Bayer Fellowship, Bayer Science & Education Foundation), and A.E. (Fundación Alfonso Martín Escudero) are gratefully appreciated. We thank Drs. D. H. Huang (TSRI), L. Pasternack (TSRI), and Q. Kleerekoper (Rice) for NMR spectroscopic, Drs. G. Siuzdak (TSRI) and C. Pennington (Rice) for mass spectrometric, and Dr. J. Korp (University of Houston) for X-ray crystallographic assistance. The National Cancer Institute (NCI) Developmental Therapeutics Program (DTP) is acknowledged for performing the in vitro screening. Part of this work was carried out at The Scripps Research Institute (TSRI). C.F.A., C.A.C., and C.E. participated at TSRI only; K.C.N., C.N., C.R.H.H., and A.E. participated at both TSRI and Rice University.

■ REFERENCES

(1) (a) Yudin, A. K. *Chem. Sci.* **2015**, *6*, 30−49. (b) Giordanetto, F.; Kihlberg, J. *J. Med. Chem.* **2014**, *57*, 278−295. (c) Heinis, C. *Nat. Chem. Biol.* **2014**, 696−698. (d) Marsault, E.; Peterson, M. L. *J. Med. Chem.* **2011**, *54*, 1961−2004. (e) Driggers, E. M.; Hale, S. P.; Lee, J.; Terrett, N. K. *Nat. Rev. Drug Discovery* **2008**, *7*, 608−624. (f) Nicolaou, K. C.; Montagnon, T. *Molecules That Changed the World*; Wiley: Weinheim, 2008. (g) Newman, D. J.; Cragg, G. M. *J. Nat. Prod.* **2012**, *75*, 311−335.

(2) (a) Nicolaou, K. C.; Snyder, S. A. *Classics in Total Synthesis II*; Wiley: Weinheim, 2003. (b) Nicolaou, K. C.; Chen, J. S. *Classics in Total Synthesis III*; Wiley: Weinheim, 2011. (c) Nicolaou, K. C.; Hale, C. R. H.; Nilewski, C.; Ioannidou, H. A. *Chem. Soc. Rev.* **2012**, *41*, 5185−5238. (d) Cragg, G. H.; Newman, D. J. *Biochim. Biophys. Acta* **2013**, *1830*, 3670−3695. (e) Goss, R. J. M.; Shankarb, S.; Abou Fayad, A. *Nat. Prod. Rep.* **2012**, *29*, 870−889. (f) McCauley, J. A.; McIntyre, C. J.; Rudd, M. T.; Nguyen, K. T.; Romano, J. J.; Butcher, J. W.; Gilbert, K. F.; Bush, K. J.; Holloway, M. K.; Swestock, J.; Wan, B.-L.; Carroll, S. S.; DiMuzio, J. M.; Graham, D. J.; Ludmerer, S. W.; Mao, S.-S.; Stahlhut, M. W.; Fandozzi, C. M.; Trainor, N.; Olsen, D. B.; Vacca, J. P.; Liverton, N. J. *J. Med. Chem.* **2010**, *53*, 2443−2463.

(3) Nicolaou, K. C.; Adsool, V. A.; Hale, C. R. H. *Angew. Chem., Int. Ed.* **2011**, *50*, 5149−5152.

(4) Nicolaou, K. C.; Hale, C. R. H.; Ebner, C.; Nilewski, C.; Ahles, C. F.; Rhoades, D. *Angew. Chem., Int. Ed.* **2012**, *51*, 4726−4730.

(5) (a) Shoemaker, R. H. *Nat. Rev. Cancer* **2006**, *6*, 813−823. (b) For the website for the National Cancer Institute Developmental Therapeutics Program (DTP NCI/NIH), see: http://www.dtp.nci.nih.gov, accessed January 9, 2015.

(6) CCDC-1033854 contains the crystallographic coordinates for compound *anti*-**26**. These data have been deposited in the Cambridge Crystallographic Data Centre (CCDC) and are freely available at: www.ccdc.cam.ac.uk.

(7) (a) Chandel, N. S. *BMC Biol.* **2014**, *12*, 34 Open Access DOI: 10.1186/1741-7007-12-34. (b) Yang, L.; Moss, T.; Mangala, L. S.; Marini, J.; Zhao, H.; Wahlig, S.; Armaiz-Pena, G.; Jiang, D.; Achreja, A.; Win, J.; Roopaimoole, R.; Rodriguez-Aguayo, C.; Mercado-Uribe, I.; Lopez-Berestein, G.; Liu, J.; Tsukamoto, T.; Sood, A. K.; Ram, P. T.; Nagrath, D. *Mol. Syst. Biol.* **2014**, *10*, 728 Open Access DOI: 10.1002/msb.20134892. (c) Caneba, C. A.; Yang, L.; Baddour, J.; Curtis, R.; Win, J.; Hartig, S.; Marini, J.; Nagrath, D. *Cell Death Dis.* **2014**, *5*, e1302 Open Access DOI: 10.1038/cddis.2014.264. (d) Anso, E.; Mullen, A. R.; Felsher, D. W.; Mates, J. M.; DeBerardinis, R. J.; Chandel, N. S. *Cancer Metab.* **2013**, *1*, 7 Open Access DOI: 10.1186/2049-3002-1-7.

(8) (a) Brand, M. D.; Nicholis, D. G. *Biochem. J.* **2011**, *435*, 297−312. (b) Wise, D. R.; Thompson, C. B. *Trends Biochem. Sci.* **2010**, *35*, 427−433.

(9) The measurement of the extracellular acidification rate (ECAR) indicated an increase of this parameter (**28**: 3.2 mpH/min/μg protein) confirming also the hyperglycolysis effect (see Supporting Information).

(10) (a) Pramanik, K. C.; Boreddy, S. R.; Srivastava, S. K. *PLoS One* **2011**, *6* (5), e20151 Open Access DOI: 10.1371/journal.pone.0020151. (b) Indran, I. R.; Tufo, G.; Pervaiz, S.; Brenner, C. *Biochim. Biophys. Acta* **2011**, *1807*, 735−745.

(11) (a) Saelens, X.; Festjens, N.; Walle, L. V.; van Gurp, M.; van Loo, G.; Vandenabeele, P. *Oncogene* **2004**, *23*, 2861−2874. (b) Mita, A. C.; Mita, M. M.; Nawrocki, S. T.; Giles, F. J. *Clin. Cancer Res.* **2008**, *15*, 5000−5005.

DOI: 10.1021/jacs.5b00141
J. Am. Chem. Soc. 2015, 137, 4766−4770